Cancer Research

Paxillin Binding to the Cytoplasmic Domain of CD103 Promotes Cell Adhesion and Effector Functions for CD8$^+$ Resident Memory T Cells in Tumors

Ludiane Gauthier[1], Stéphanie Corgnac[1], Marie Boutet[1], Gwendoline Gros[1], Pierre Validire[2], Georges Bismuth[3], and Fathia Mami-Chouaib[1]

Abstract

CD8$^+$/CD103$^+$ tissue-resident memory T cells (T_{RM} cells) accumulate in several human solid tumors, where they have been associated with a favorable prognosis. However, the role of CD103, the α subunit of the integrin $\alpha_E\beta_7$ (also known as CD103), in the retention and functions of these T_{RM} is undefined. In this report, we investigated the role of CD103 cytoplasmic domain and the focal adhesion-associated protein paxillin (Pxn) in downstream signaling and functional activities triggered through α_E/CD103 chain. Binding to immobilized recombinant (r)E-cadherin-Fc of CD103 integrin expressed on tumor-specific CTL clones promotes phosphorylation of Pxn and Pyk2 and binding of Pxn to the α_E/CD103 subunit tail. Inhibition of Pxn phosphorylation by the Src inhibitor saracatinib or its knockdown via shRNA dramatically altered adhesion and spreading of freshly isolated CD8$^+$/CD103$^+$ lung tumor–infiltrating lymphocytes and CD103$^+$ tumor-specific CTL clones. Inhibition of Pxn phosphorylation with saracatinib in these CTL clones also severely compromised their functional activities toward autologous tumor cells. Using Jurkat T cells as a model to study CD103 integrin activation, we demonstrated a key role of serine residue S1163 of the α_E chain intracellular domain in polarization of CD103 and recruitment of lysosomes and Pxn at the contact zone of T lymphocytes with rE-cadherin-Fc–coated beads. Overall, our results show how Pxn binding to the CD103 cytoplasmic tail triggers $\alpha_E\beta_7$ integrin outside-in signaling that promotes CD8$^+$ T-cell migratory behavior and effector functions. These results also explain the more favorable prognosis associated with retention of T_{RM} cells in the tumor microenvironment. *Cancer Res; 77(24); 7072–82.* ©*2017 AACR.*

Introduction

The α_E(CD103)β_7 integrin, hereafter referred to as CD103, plays a key role in cytotoxic immunological synapse (IS) formation and T-cell receptor (TCR)–mediated cytotoxicity toward epithelial tumor cells, through polarized exocytosis of their lytic granules at the IS (1, 2). CD103 defines a novel subtype of memory CD8$^+$ T cells, called tissue resident memory T (T_{RM}) cells, that stably reside in peripheral non-lymphoid tissues, including lung, gut, and skin, where they orchestrate a highly protective local immune response to persistent viral infections (3–6) and probably also toward cancer cells. This CD103$^+$ T_{RM} subset, which likely derives from tissue-recruited effector T (T_{Eff}) cells, is defined by a CD69^{high}/CCR7^{low}/S1PR1^{low} profile and expression of transcription factors Hobit and Blimp1, that cooperate to repress genes involved in tissue egress, including *ccr7* and *S1pr1* (7, 8). Accumulating evidence now indicates that CD8$^+$/CD103$^+$ T_{RM} cells ostensibly play a central role in antitumor T-cell immunity. Indeed, a correlation between tumor infiltration by CD103$^+$ tumor-infiltrating lymphocytes (TIL) and patient survival has been established in many malignant diseases, including ovarian, lung, endometrial, and breast cancers (9–12). CD103 promotes CD8$^+$ TIL activities by mediating T-cell recruitment within epithelial tumor islets, and initiating intratumoral early T-cell signaling (13). This integrin also controls CD3$^+$/CD8$^+$ TIL functions, not only by inducing T-cell adhesion to cancer cells upon interaction with its ligand, the epithelial cell marker E-cadherin on target cells, but also by triggering bi-directional signaling events that cooperate with TCR signals to enable tumor cell killing by specific CTL (13, 14). In this context, it is therefore crucial to understand the mechanisms behind the signaling properties of the CD103 integrin.

After recognition by specific CTL of MHC class I antigenic peptide complexes on target cells, microclusters are generated before IS formation in which TCR and signaling molecules

[1]INSERM UMR 1186, Integrative Tumor Immunology and Genetic Oncology, Gustave Roussy, EPHE, Fac. de médecine - Univ. Paris-Sud, Université Paris-Saclay, Villejuif, France. [2]Service d'Anatomie Pathologique, Institut Mutualiste Montsouris, Paris, France. [3]INSERM U1016, CNRS UMR8104, Université Paris Descartes, Institut Cochin, Paris, France.

Note: Supplementary data for this article are available at Cancer Research Online (http://cancerres.aacrjournals.org/).

S. Corgnac, M. Boutet, and G. Gros contributed equally to this article.

Current address for M. Boutet: Department of Microbiology and Immunology Albert Einstein College of Medicine, New York, NY.

Corresponding Author: Fathia Mami-Chouaib, Gustave Roussy, 114, rue Edouard Vaillant, 94805 Villejuif, France. Phone: 331-4211-4965; Fax: 331-4211-5288; E-mail: fathia.mami-chouaib@gustaveroussy.fr

doi: 10.1158/0008-5472.CAN-17-1487

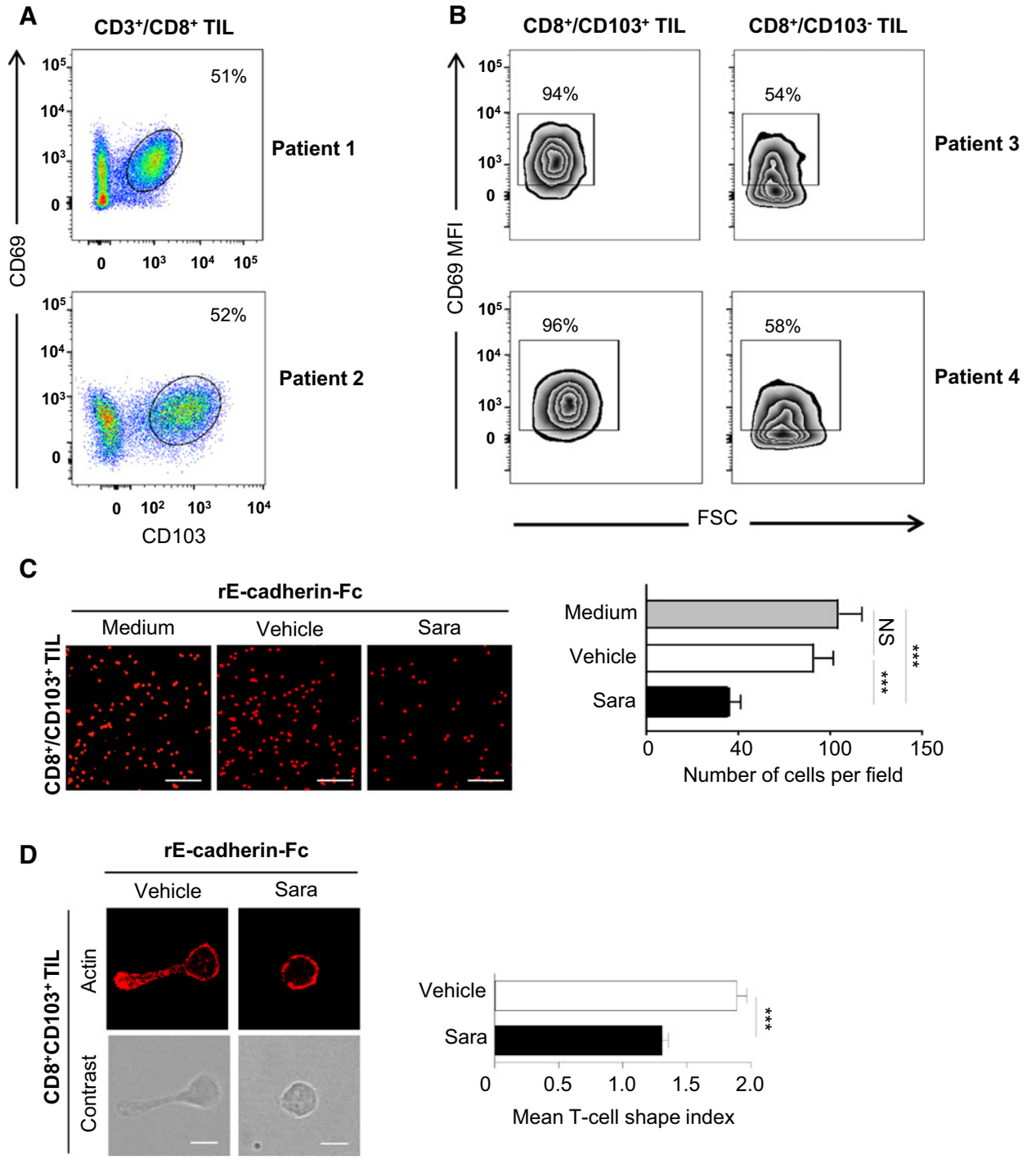

Figure 1.

The src inhibitor saracatinib (Sara) inhibits adhesion and spreading of freshly isolated lung tumor T_{RM} cells. **A,** Expression of CD103 and CD69 T_{RM} markers on NSCLC $CD3^+/CD8^+$ TIL. Freshly resected NSCLC tumors were dissociated, and the CD8 T-cell subset was positively selected and then directly analyzed by flow cytometry for CD69 and CD103 expression. Two representative TIL samples used in this study are shown. Percentages of $CD103^+/CD69^+$ among $CD3^+/CD8^+$ cells are indicated. **B,** Expression of CD69 activation marker on freshly isolated $CD8^+/CD103^+$ and $CD8^+/CD103^-$ TIL. Two representative TIL samples are shown. Percentages of $CD69^+$ cells are included. **C,** Saracatinib inhibits adhesion of freshly isolated NSCLC T_{RM} to rE-cadherin-Fc. Adhesion to plastic-bound rE-cadherin-Fc of freshly isolated $CD8^+/CD103^+$TIL, untreated (medium) or pretreated with saracatinib or vehicle control (DMSO), was analyzed by confocal microscopy. Right, Mean numbers of adherent lymphocytes per field. Adhesion was evaluated by counting adherent lymphocytes stained with CD103 and DAPI. Statistical analyses are from three independent experiments; scale bars, 100 μm; ***, $P < 0.0001$. **D,** Migratory behavior of freshly isolated TIL T_{RM} on immobilized rE-cadherin-Fc. $CD8^+/CD103^+$ TIL, untreated or pretreated with saracatinib, were seeded on rE-cadherin-Fc and polymerized F-actin was visualized with rhodamine phalloidin. Right, Mean T-cell shape index. Statistical analyses are from three independent experiments; scale bars, 5 μm; ***, $P < 0.0001$.

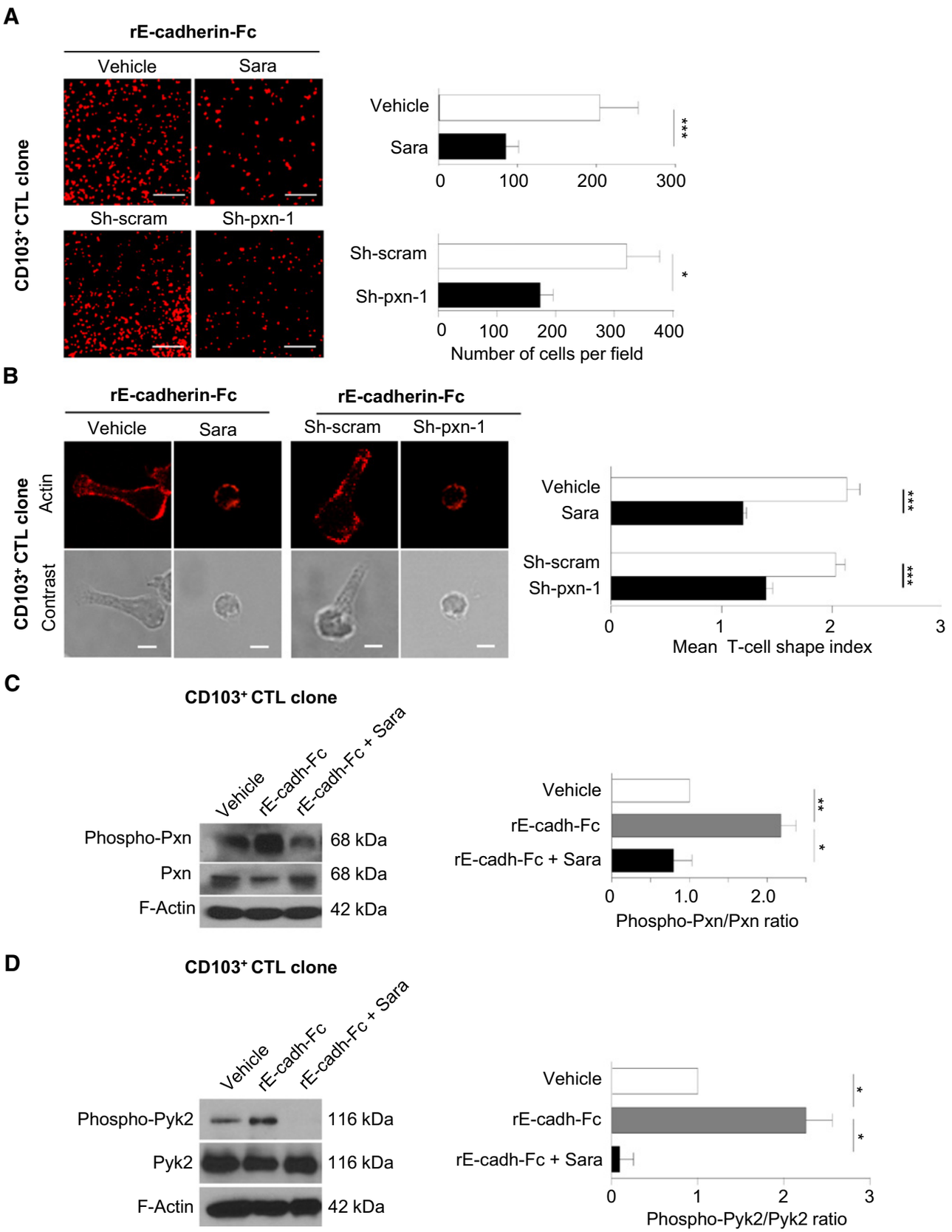

assemble at the interface between the two cell types. Each TCR microcluster is surrounded by an adhesion molecule structure, including leukocyte-function-associated antigen (LFA-1), the focal-adhesion–associated adaptor protein paxillin (Pxn) and proline-rich tyrosine kinase-2 (Pyk2). Disruption of these microstructures by downregulating both Pxn and Pyk2 inhibits T-cell activation and functions, indicating that these molecules are necessary for providing the outside-in signals required for optimal CTL responses (15, 16). Pxn is a 68 kDa protein associated with actin binding and signaling proteins. This adaptor molecule is activated through phosphorylation of several tyrosine (Tyr^{31} and Tyr^{118}) and serine (Ser^{85} and Ser^{178}) residues by different kinases, including focal adhesion kinase (FAK), Src kinase, JNK, and p38 MAPK (17–19). Phosphorylated (phospho)-Pxn participates in TCR-mediated CTL activation through an integrin-dependent mechanism (20–22). Moreover, binding of Pxn to the α_4 integrin cytoplasmic tail promotes an outside-in costimulatory signal that participates in integrin-mediated T-cell migration (23, 24). A mutation (E983A or Y991A) in the α_4 cytoplasmic tail selectively blocks the interaction with Pxn and thus reduces T-cell spreading.

In this report, we investigated the role of the intracellular domain of the α_E subunit in signaling and downstream functions of the CD103 integrin, and the involvement of Pxn in these processes. Our data show that the interaction of CD103 with its ligand E-cadherin promotes phosphorylation of Pxn and Pyk2 and binding of Pxn to the α_E chain cytoplasmic domain. Our data also indicate the key role of serine residue S^{1163} in the α_E cytoplasmic tail in CD103 integrin-mediated T-cell functions. Indeed, an S1163A mutation abrogates relocalization of CD103 at the contact zone between T cells and rE-cadherin-Fc–coated beads and inhibits the secretory lysosome and Pxn polarization. Thus, the CD103-Pxn partnership is likely to represent a major outside-in signaling axis required for effector functions of CTL, including T_{RM}, and thereby opens new avenues for the success of T-cell–based cancer immunotherapies.

Materials and Methods

Tumor cell lines, T cells, and freshly isolated lung TIL T_{RM}

The IGR-Heu tumor cell line was established in one of our laboratories in 1996 from a non–small cell lung carcinoma (NSCLC) as described (1). Heu171 and H32-8 T-cell clones, generated from autologous TIL and PBL, respectively, recognized a mutated α-actinin-4 tumor neoepitope (25). Cells were regularly tested and authenticated by immunofluorescence analysis and cytotoxic assay, including in the present work.

A JTag clone, stably transfected with the SV40 large T antigen, was derived from the human leukemia $CD4^+$ Jurkat T-cell line. JTag cells were cloned by limiting dilution and an α_E^-/β_7^+ JTag T-cell clone was selected.

Fresh human NSCLC tumors were obtained from the Institut Mutualiste Montsouris (Paris) and immediately dissociated mechanically and enzymatically using a tumor dissociation kit (MACS, Miltenyi Biotec). Mononuclear cells were then isolated by a Ficoll-Hypaque gradient, and CD8 T cells were positively selected using CD8 microbeads according to the manufacturer's instructions (Miltenyi Biotec).

Recombinant molecules, antibodies, and chemical inhibitor

The human rE-cadherin-Fc molecule was provided by R&D Systems. Anti-CD103 (2G5) mAb was purchased from Beckman Coulter and PE-conjugated anti-CD103 was purchased from eBiosciences. Anti-CD3 (UCHT1) was provided by Ozyme and anti-CD8 (RPA-T8) was supplied by BioLegend. Anti-Pxn and anti-phospho-Pxn (Tyr118) mAb were purchased from BD Biosciences and Cell Signaling Technology, respectively. Anti-Pyk2 and anti–phospho-Pyk2 (Tyr 402) were purchased from Life Technologies.

The src inhibitor, saracatinib (AZD0530), was purchased from Millipore.

Production of Pxn shRNA lentivirus and T-cell transfection

Two shRNA targeting human Pxn (sh-pxn-1: GGGCAGCAACCTTTCTGAACT and sh-pxn-2: GATCCCGGCAAGGACTACTTCGACATGT) were synthesized (Sigma Aldrich) and then inserted into a pBlue Script containing the human H1 promoter. A scrambled sequence (CGGCAGCTAGCGACGCCAT) was also synthesized and used as a negative control. The *H1*-pxn-1, *H1*-pxn-2 and *H1*-scrambled cassettes were inserted into the linearized pRRLsin-PGK-eGFP-WPRE viral vector. Lentivirus particles were prepared by transient cotransfection of HEK293T cells (human 293 embryonic kidney cells transformed with the SV40 large T-antigen) with lentiviral vector plasmids (sh-pxn-1, sh-pxn-2 or sh-scrambled), packaging plasmid pCMVΔR8.91 and the pMD2.G protein envelope plasmid. JetPrime was used for transfection of HEK293T according to the manufacturer's instructions (Ozyme). Briefly, lentivirus particles were immediately added to give a multiplicity of infection (MOI) of 30, spinoculated for 1 hour at 1,300 rpm, and then lymphocytes were cultured in the presence of IL-2 (50 U/mL) for 3 days.

Figure 2.

CD103 integrin promotes adhesion and spreading of $CD8^+/CD103^+$ CTL in a Pxn-dependent pathway. **A,** Adhesion of $CD8^+/CD103^+$CTL on a rE-cadherin-Fc monolayer. Adhesion to plate-bound rE-cadherin-Fc of the $CD8^+/CD103^+$ T-cell clone H32-8, untreated (DMSO) or pretreated with saracatinib (Sara) or infected with sh-pxn-1 or sh-scrambled (sh-scram) negative control. Right, Mean numbers of adherent lymphocytes per field. Statistical analyses are from three independent experiments; bars, 100 μm and *, $P < 0.05$; ***, $P < 0.0001$. **B,** Migratory behavior of $CD8^+/CD103^+$CTL on rE-cadherin-Fc monolayer. The $CD8^+/CD103^+$ H32-8 T-cell clone, untreated (vehicle) or pretreated with saracatinib or infected with sh-pxn-1, was seeded on immobilized rE-cadherin-Fc and then cell shape was monitored. Sh-scrambled was used as a negative control. Polymerized F-actin was visualized with rhodamine phalloidin. Right, mean T-cell shape index. Statistical analyses are from three independent experiments; scale bars, 5 μm; ***, $P < 0.0001$. **C,** Interaction of CD103 with its ligand E-cadherin triggers phosphorylation of Pxn, which is inhibited by saracatinib. The $CD8^+/CD103^+$ T-cell clone H32-8, untreated (vehicle control) or preatreated with saracatinib, was stimulated with immobilized rE-cadherin-Fc (E-cadh-Fc), and then protein extracts were analyzed by Western blot using anti–phospho-Pxn, anti-Pxn, or anti–F-actin mAb. Right, normalization of phospho-Pxn relative to total Pxn. Data shown are from three independent experiments; *, $P < 0.05$ and **, $P < 0.001$. **D,** Interaction of CD103 with E-cadherin triggers phosphorylation of Pyk2, which is inhibited by saracatinib. The $CD8^+/CD103^+$ T-cell clone H32-8, untreated (vehicle) or preatreated with saracatinib, was stimulated with plastic-bound rE-cadherin-Fc and then protein extracts were analyzed by Western blot using anti–phospho-Pyk2, anti-Pyk2, or anti–F-actin mAb. Right, normalization of phospho-Pyk2 relative to total Pyk2. Data shown are from three independent experiments; *, $P < 0.05$.

Confocal microscopy and quantification of protein polarization

For T-cell adhesion, poly-L-lysine slices were coated with rE-cadherin-Fc (5 μg/mL) overnight at 4°C, and lymphocytes, untreated or treated for 4 hours with saracatinib (4 μmol/L) or infected with specific shRNA (sh-pxn-1, sh-pxn-2 or sh-scrambled) were incubated for 1 hour at 37°C. Cells were then fixed and permeabilized and polymerized F-actin was stained with rhodamine phalloidin as described (1, 13). Cell shape index was calculated as the ratio of the longest to the shortest axis measured via ImageJ software as described previously (13).

For protein polarization, T cells, untreated or pretreated with saracatinib or sh-RNA or transfected with CD103-GFP constructs, were pre-incubated for 30 minutes with rE-cadherin-Fc–coupled protein G-Dynabeads or IGR-Heu tumor cells, at a 2:1 effector to target cell (E:T) ratio and then plated on poly-(L-lysine)–coated coverslips. Cells were then fixed, permeabilized and stained with mouse anti-CD103 or mouse anti-Pxn mAb, followed by anti-mouse-Alexa-Fluor-488. Coverslips were mounted and analyzed using a fluorescence microscope with x63 lenses as described previously (1, 13). To quantify polarization of the proteins to the IS with target cells or the contact zone with E-cadherin-Fc–coated beads, a volume corresponding to the synaptic area and an equal volume at the opposite site of the T cell were drawn and fluorescence intensities (FI) were calculated. Results were reported as the fold-increase in the corresponding staining integrated FI at the synaptic region, divided by the same FI measured at the distal region (26).

Western blot and immunoprecipitation experiments

T cells (5×10^5), untreated or pretreated with saracatinib or shRNA, were unstimulated or stimulated for 10 minutes at 37°C with plastic-coated rE-cadherin-Fc. Total protein extracts were obtained by cell lysis in ice-cold lysis buffer supplemented with a cocktail of anti-proteases and anti-phosphatases as described previously (14). Equivalent amounts of protein extracts were denatured, separated by SDS-PAGE and transferred to a nitrocellulose membrane. Blots were incubated for 30 minutes in Tris-buffered saline containing 0.1% Tween 20 and 5% nonfat dry milk, and further incubated overnight at 4°C with rabbit anti-phospho-Pxn, anti-Pxn, anti-phospho-Pyk-2 and anti–Pyk-2 mAb, followed by appropriate secondary horseradish peroxidase–conjugated Ab.

For immunoprecipitation, T-cell extracts were incubated for 2 hours at 4°C with cross-linked anti-CD103 or anti-Pxn beads, or protein G-sepharose beads prebound with control mouse IgG. Beads were then washed and eluted with reducing agent at 95°C.

Construction of CD103–GFP fusion proteins and transfection of JTag cells

An *ITGAE* cDNA coding for the human α_E (CD103) subunit, cloned in a pAMR8 vector (27), was a gift from Prof. Michael B. Brenner (Boston, MA). The cDNA clone was subcloned in pEGFPN1 plasmid and fused to GFP by directed mutagenesis (CD103-WT-GFP). Deletions in CD103 cytoplasmic domains were generated with the Quickchange II XL Site-Directed Mutagenesis Kit (Agilent Technologies). The CD103–WT–GFP construct was used to generate CD103-Δ1 with forward 5′-GTGTGGCTTTTTTAAAAGAAAACTCAAGCTTCGAATTCTGCAGTC-3′ and reverse 3′-GACTGCAGAATTCGAAGCTTGAGTTTTCTTTTAAAAAAGCCACAC-5′ primer pairs; CD103-Δ2 with forward 5′-GAAAATATCAACAACTGAACTTGCTCAAGCTTCGAATTCTGCAG-3′ and reverse 5′-CTGCAGAATTCGAAGCTTGAGCAAGTTCAGTTGTTGATATTTTC-3′; CD103-Δ3 with forward 5′-GAGCATCAGGAAGGCCCAGCTGCTCAAGCTTCGAATTCTG-3′ and reverse 5′-CAGAATTCGAAGCTTGAGCAGCTGGGCCTTCCTGATGCTC-3′; CD103-Y1156A with forward 5′-GTGTGGCTTTTTTAAAAGAAAAGCACAACAACTGAACTTGGAGGC-3′ and reverse 5′-GCCTCCAAGTTCAGTTGTTGTGCTTTTCTTTTAAAAAAGCCACAC-3′. CD103-S1163A with forward 5′-AGCTGGGCCTTCCTGATTGCCTCCAAGTTCAGTTGTTG-3′ and reverse 5′- CAACAACTGAACTTGGAGGCAATCAGGAAGGCCCAGCT-3′; and CD103-S1163D with forward 5′-AGCTGGGCCTTCCTGATGTCCTCCAAGTTCAGTTGTTG-3′ and reverse: 5′-CAACAACTGAACTTGGAGGACATCAGGAAGGCCCAGCT-3′ primer pairs. The CD103-S1163A construct was used to generate CD103-Y1156A/S1163A with forward 5′-GTGTGGCTTTTTTAAAAGAAAAGCACAACAACTGAACTTGGAGGC-3′ and reverse 5′-GCCTCCAAGTTCAGTTGTTGTGCTTTTCTTTTAAAAAAGCCACAC-3′.

Ten × 10^6 β_7^+ JTag cells were resuspended in RPMI supplemented with 10% heat-inactivated FBS with 30 μg of plasmid DNA and transferred to a 0.4-cm electroporation cuvette. Electroporation was performed with the Gene Pulser II system (Bio-Rad Laboratories) at 280 V and 900 μF; next, cells were cultured in fresh complete medium for 48 hours.

Functional experiments

Cytotoxicity of T-cell clones was evaluated with a conventional 4 hours ^{51}Cr-release assay. T cells were either kept in medium or treated with saracatinib; then, cytotoxic activity toward autologous IGR-Heu tumor cells was determined at a 30:1, 10:1, 3:1 E:T ratios.

For cytokine release, H32-8 T cells (3×10^3/well), untreated or pretreated with saracatinib, were cocultured in the presence of IGR-Heu (3×10^4/well) for 24 hours and then, IFNγ production in culture supernatants was measured by ELISA (eBioscience).

For T-cell recruitment, xenograft tumor samples were embedded in low-gelling-temperature agarose and lymphocytes, untreated or pretreated with saracatinib and stained with SNARF, were added onto the cut surface of each slice as described (13). Images were acquired with a ×4 or ×10 (S fluor; Nikon) objective and MetaVue imaging software (Universal Imaging).

For single-cell calcium measurement, JTag cells were labeled with 1 μmol/L Fura-2AM (Molecular Probes), and alternatively excited every 10 s at 350 and 380 nm on an inverted Eclipse TE300 microscope equipped with a ×10 objective and a Metafluor imaging system. At 60 s, rE-cadherin-Fc (5 μg/mL) plus anti–CD3 (0.5 μg/mL)-coated beads were added. Values were represented as a ratio of FI at 350 nm/FI at 380 nm.

Statistical analysis

Statistical significance was determined with the one-way ANOVA test with Bonferroni correction or with the two-tailed Student *t* test (GraphPad Prism, GraphPad software).

Results

Pxn is involved in CD103-mediated adhesion and spreading of $CD8^+$ T_{RM} cells from human lung tumors

To investigate the contribution of adapter protein Pxn to CD103-mediated T-cell functions, we first tested the effect of the

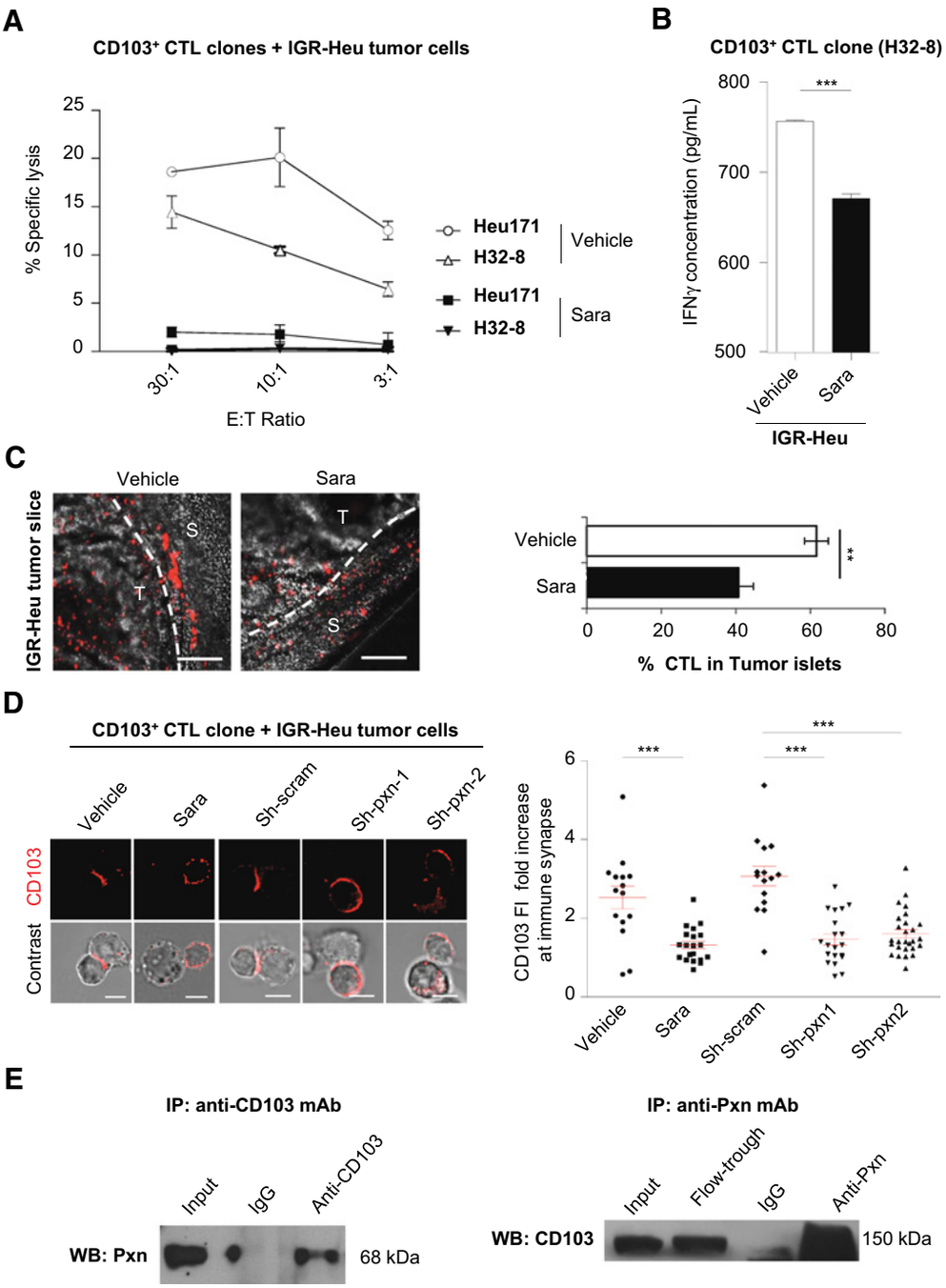

Figure 3.

Pxn binds to the CD103 tail and controls CD103-dependent signaling and T_{RM} functions. **A,** Cytotoxicity of $CD8^+/CD103^+$ CTL clones toward specific tumor cells was inhibited with saracatinib (Sara). Heu171 and H32-8 ($CD103^+/LFA\text{-}1^+$) CTL clones were untreated (vehicle control) or pretreated with saracatinib, then cytotoxicity toward autologous IGR-Heu (E-cadherin$^+$/ICAM-1$^-$) tumor cells was measured by a chromium release assay. **B,** Cytokine release by $CD8^+/CD103^+$ CTL was inhibited with saracatinib. The $CD103^+$ H32-8 CTL clone, untreated or pretreated with saracatinib, was stimulated for 24 hours with autologous IGR-Heu cells and then IFNγ release in culture medium was measured by ELISA; **, $P < 0.01$. **C,** Recruitment of fluorescent-labeled $CD103^+$ H32-8 lymphocytes, untreated or pretreated with saracatinib, within epithelial tumor regions of human lung tumor (IGR-Heu) slices. Stromal (S) and tumor (T) areas were identified by brightness contrast. Right, percentages of T cells inside tumor areas were determined from two independent experiments; bars, 100 μm; **, $P < 0.01$. **D,** Polarization of CD103 at the IS is inhibited by saracatinib- and shRNA-targeting Pxn. The H32-8 T-cell clone, untreated or pretreated with saracatinib or infected with sh-pxn-1 or sh-pxn-2, was cocultured with autologous IGR-Heu target cells and then CD103 relocalization at the IS was analyzed by confocal microscopy. Vehicle alone and sh-scrambled (sh-scram) were used as negative controls, respectively. Right, CD103 fluorescence intensity (FI) fold increase at the IS with target cells ($n = 40$). Red horizontal lines correspond to the mean fold increase ± SEM. Statistical analyses are from two independent experiments; scale bars, 5 μm; ***, $P < 0.0001$. **E,** Pxn binds to the α_E subunit tail. Protein extracts from the $CD8^+/CD103^+$H32-8 clone, stimulated with immobilized rE-cadherin-Fc for 30 minutes, were immunoprecipitated (IP) using anti-CD103 mAb and then immunoblotted (WB, Western blot) with anti-Pxn. An IgG negative control was included. Right, protein extracts from the $CD8^+/CD103^+$ T-cell clone, stimulated with plastic-bound rE-cadherin-Fc, were immunoprecipitated (IP) by anti-Pxn mAb and then immunoblotted (WB, Western blot) with anti-CD103.

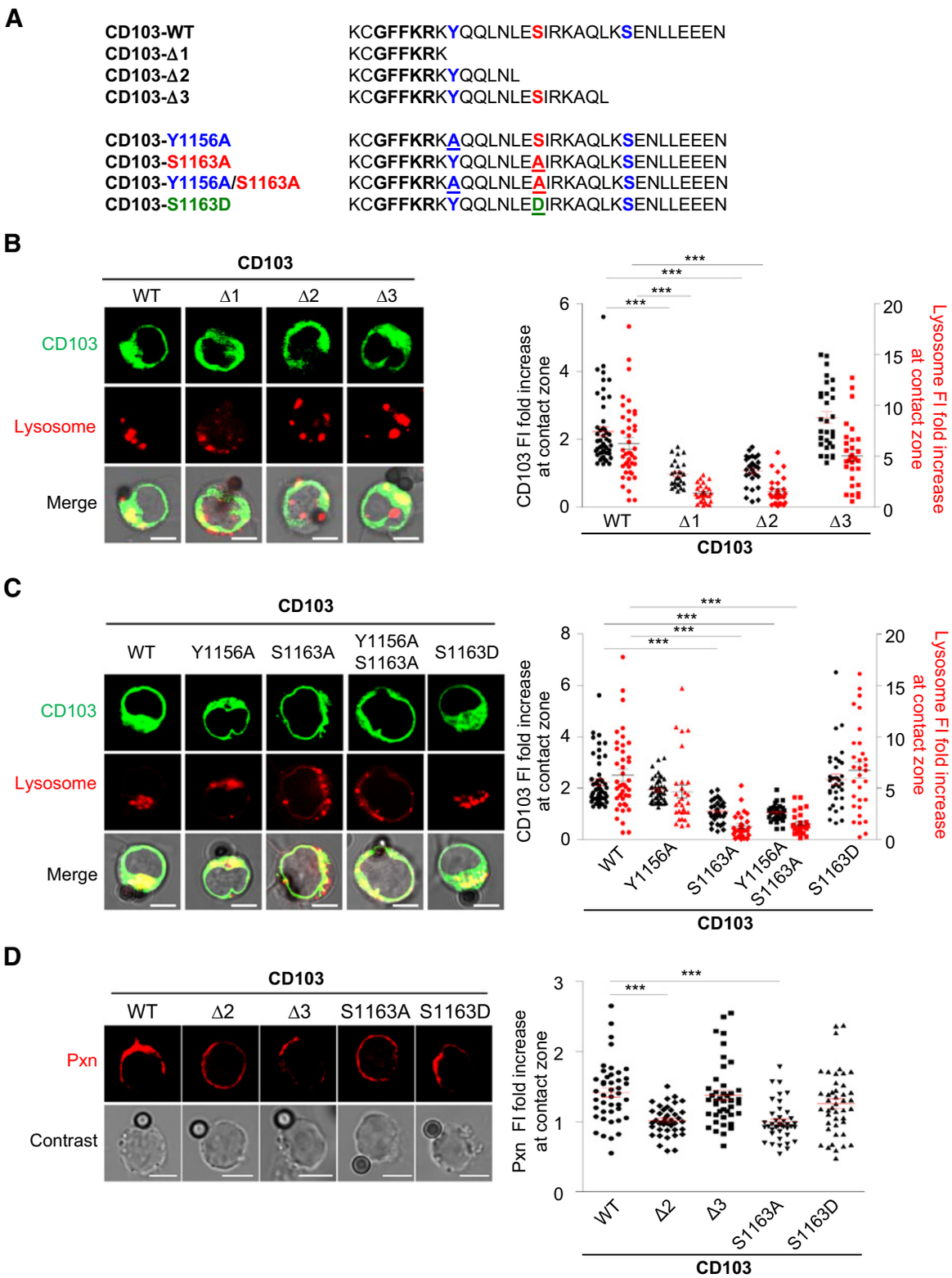

Src inhibitor saracatinib (AZD0530) on the adhesion and migratory behavior of $CD8^+/CD103^+$ T_{RM} cells freshly isolated from human lung tumors. In these tumors, the $CD8^+/CD103^+$ T_{RM} subset frequently represents around half of the total $CD3^+/CD8^+$ T cells, and most of them expressed activation marker CD69 (Fig. 1A) as compared with $CD8^+/CD103^-$ TIL (Fig. 1B). Results indicated that saracatinib inhibited adhesion and spreading of freshly isolated $CD8^+/CD103^+$ T_{RM} cells on a human recombinant (r) E-cadherin-Fc (rE-cadherin-Fc) monolayer (Fig. 1C and D). In contrast, vehicle control (DMSO) had no effect. Similar effects of saracatinib were obtained with the tumor-specific H32-8 T-cell clone (Fig. 2A and B) and the Heu171 TIL clone (Supplementary Fig. S1A and S1B), with both displaying a typical $CD3^+/CD8^+/CD103^+/CD69^+/CD27^-/CD28^-/CD62L^-/CCR7^-$ T_{RM} phenotype (28).

Next, we tested whether CD103 engagement on the H32-8 $CD8^+/CD103^+$ T-cell clone with plastic-coated rE-cadherin-Fc was able to induce phosphorylation of Pxn, and how saracatinib could affect this phosphorylation. Western blot analyses with a phospho-Pxn-specific monoclonal antibody (mAb) revealed that ligation of CD103 on T-cell clone H32-8 triggered phosphorylation of Pxn, and this phosphorylation was inhibited by saracatinib (Fig. 2C). Ligation of CD103 on the CTL clone also triggered phosphorylation of the binding partner of Pxn, Pyk2 tyrosine kinase, which was abrogated by saracatinib (Fig. 2D). Then, and to directly address the role of Pxn, we used two short hairpin (sh)RNA (sh-pxn-1 and sh-pxn-2) targeting the *PXN* gene (Supplementary Fig. S1C). Results indicated that Pxn knockdown impaired T-cell adhesion and spreading on plate-bound rE-cadherin-Fc of the $CD103^+$ CTL clone H32-8 (Fig. 2A and B). Similar results for T-cell adhesion were obtained with $CD8^+/CD103^+$ T cells generated from healthy donor peripheral blood lymphocytes (PBL) after treatment with a combination of TGF-β plus anti-CD3 mAb (Supplementary Fig. S1D; ref. 29). In these experiments, we verified that neither saracatinib nor sh-pxn had an effect on T-cell viability (Supplementary Fig. S2A and S2B) or cell surface expression of CD3, CD8, and CD103 (Supplementary Fig. S2C and S2D). Saracatinib had also no effect on cell surface expression of PD-1 and Tim-3 molecules on $CD8^+/CD103^+$ TIL (Supplementary Fig. S2E). These results demonstrated that Pxn is involved in CD103 intracellular signaling and CD103-mediated T_{RM} cell adhesion and spreading.

Pxn binds to the CD103 cytoplasmic domain and its phosphorylation promotes $CD8^+$ T_{RM} cell functions

We then evaluated the consequences of inhibiting Pxn phosphorylation on the CD103-dependent TCR-mediated cytotoxicity of $CD8^+/CD103^+$ Heu171 and H32-8 T-cell clones toward autologous target cells. Results showed that preincubating these CTL clones with saracatinib abrogated their lytic activity toward specific IGR-Heu tumor cells (Fig. 3A). Saracatinib also inhibited IFNγ release by H32-8 CTL stimulated with autologous target cells (Fig. 3B). Moreover, experiments performed in a physiological-like condition using our previously described system based on viable IGR-Heu tumor slices (13), indicated that saracatinib inhibited recruitment of H32-8 T cells in epithelial tumor regions (Fig. 3C). Inhibition of T-cell functions correlated with inhibition of CD103 relocalization at the IS between saracatinib-treated $CD8^+/CD103^+$ H32-8 CTL and autologous $ICAM\text{-}1^-$/$E\text{-}cadherin^+$ IGR-Heu target cells (Fig. 3D). Importantly, inhibition of CD103 relocalization at the IS was also observed after knockdown of Pxn in this T-cell clone with sh-pxn-1 or sh-pxn-2 shRNA (Fig. 3D). In contrast, sh-scrambled, used as a negative control, had no effect. In these experiments, we also verified that sh-pxn had an effect on CTL clone viability (Supplementary Fig. S2B).

We next investigated whether Pxn could bind to CD103 in $CD8^+/CD103^+$ T cells. With this aim, we stimulated $CD103^+$ CTL clone H32-8 with immobilized rE-cadherin-Fc, and then performed immunoprecipitation experiments with anti-CD103 or anti-Pxn Abs. Western blot analysis of the two types of immunoprecipitates after CD103 engagement showed that a complex is formed in which the two proteins are present (Fig. 3E). These results further support the conclusion that Pxn is involved in CD103 signaling upon its binding to the CD103 intracellular domain.

The Ser^{1163} residue in the α_E tail is required for triggering CD103 clustering and outside-in signaling

The short α_E chain cytoplasmic domain of CD103 contains one Tyr (Y^{1156}) and two Ser (S^{1163} and S^{1171}) residues that could potentially be phosphorylated after CD103 engagement with its ligand E-cadherin. Studies were thus carried out to investigate their role in CD103 signaling and Pxn binding. With this aim, we first constructed several deletion mutants of the α_E subunit, containing, or not, these residues and fused to GFP (Fig. 4A, top). In these mutants, the cytoplasmic KCGFFKRK sequence of CD103

Figure 4.

The α_E subunit cytoplasmic tail is required for CD103 integrin signaling. **A,** Integrin *ITGAE*–GFP constructs encoding WT-CD103–GFP fusion protein or mutated-CD103–GFP fusion proteins containing either deletions (CD103-Δ1, CD103-Δ2 and CD103-Δ3) or punctual mutations (CD103-Y1156A, CD103-S1163A, CD103-Y1156A/S1163A, and CD103-S1163D) in the α_E subunit cytoplasmic domain. In the Δ1 construct, the entire cytoplasmic tail was deleted except for the juxtamembrane "GFFKR" domain. In the Δ2 construct, 6 aa containing Tyr^{1156} were added compared with Δ1 and 8 supplementary aa with Ser^{1163} were added in Δ3 as compared with Δ2. In the CD103-Y1156A construct, Tyr^{1156} was substituted by an Ala; in CD103-S1163A, Ser^{1163} was replaced by an Ala; and, in CD103-Y1156A/S1163A, both Tyr^{1156} and Ser^{1163} were substituted by Ala. In the CD103-S1163D construct, Ser^{1163} was replaced by Asp to mimic phosphorylation. **B,** Effects of CD103 cytoplasmic domain deletions on integrin and lysosome polarization. The α_E^-/β_7^+ JTag T-cell clone was transfected with WT-CD103-GFP or CD103-Δ1, -Δ2 or -Δ3 constructs, and then relocalization of CD103 or lysotracker at the contact zone with rE-cadherin-Fc–coated beads was analyzed by confocal microscopy. Right, CD103 and lysosome FI fold increase at the contact area with rE-cadherin-Fc–coated beads ($n = 30$). Red and black horizontal lines correspond to mean fold-increase ± SEM. Data from three independent experiments were quantified; scale bars, 5 μm; ***, $P < 0.0001$. **C,** Effect of CD103 cytoplasmic domain substitutions on integrin and lysosome polarization. JTag cells were transfected with WT-CD103-GFP, CD103-Y1156A, CD103-S1163A, CD103-Y1156A/S1163A, or CD103-S1163D constructs, and then relocalization of CD103 or the lysotracker at the contact zone with rE-cadherin-Fc–coated beads was analyzed. Right, CD103 and lysosome FI fold increase at the contact zone with rE-cadherin-Fc–coated beads ($n = 30$). Red and black horizontal lines correspond to the mean fold-increase ± SEM. Data are from three independent experiments; bars, 5μm; ***, $P < 0.0001$. **D,** Polarization of Pxn at the contact area with rE-cadherin-Fc–coated beads. JTag cells were transfected with CD103-WT or CD103-Δ2, CD103-Δ3, CD103-S1163A, or CD103-S1163D constructs, and then relocalization of Pxn at the contact zone with rE-cadherin-Fc–coated beads was analyzed. Right, Pxn FI fold increase at the IS with rE-cadherin Fc–coated beads ($n = 30$). Red horizontal lines correspond to the mean fold increase ± SEM. Data from three independent experiments were quantified; scale bars, 5 μm; ***, $P < 0.0001$.

was kept intact, because the conserved GFFKR juxta-membrane domain is required for integrin activation and interaction with the β-integrin chain through a salt bridge between the arginine residue from the α-chain and the aspartic acid residue from the HDR(R/K)E proximal domain of the β-chain (30, 31). These CD103 constructs were transfected into an α_E^-Jurkat T-cell (JTag) clone, which was previously selected for spontaneous strong expression of the integrin β_7-subunit (see Supplementary Fig. S3A) to obtain satisfactory expression of the $\alpha_E\beta_7$ heterodimer in the transfected cells. CD103 integrin clustering at the contact zone with rE-cadherin-Fc–coated beads was then analyzed by confocal microscopy as well as accumulation of lysosomes. A wild-type (WT) CD103-GFP molecule was used as a control. Compared to the control, CD103 clustering and lysosome polarization were strongly inhibited by CD103-Δ1 and CD103-Δ2 mutants (Fig. 4B). In contrast, the CD103-Δ3 mutant functioned like CD103-WT, suggesting that S^{1163}, but not S^{1171}, is essential for this activity.

To further verify this hypothesis, we constructed four additional mutants containing single amino acid (aa) substitutions of S^{1163} and/or Y^{1156} to alanine (Fig. 4A, bottom). We found that only the substitution of S^{1163} (S1163A) resulted in loss of integrin clustering and lysosome polarization (Fig. 4C). As expected, a construct containing both substitutions had similar effects. Moreover, substitution of the Ser by an aspartate (D) at position 1163 (CD103-S1163D), to mimic phosphorylation, restored CD103 clustering and lysosome relocalization. We controlled, in these experiments, that JTag cells transfected with the different CD103–GFP fusion proteins displayed similar expression levels of CD103. For unexplained reasons, only the CD103–S1163D protein was expressed at lower levels (Supplementary Fig. S3B). All transfectants also displayed the same capacity to adhere to plastic-bound rE-cadherin-Fc (Supplementary Fig. S3C) and to form conjugates with rE-cadherin-Fc-coated beads (Supplementary Fig. S3D). These results further support the conclusion that the phosphorylation status of S^{1163} in the α_E-ESIRKAQL intracellular motif is crucial for CD103 clustering and outside-in signaling.

The α_E-Ser^{1163} residue is required for triggering Pxn polarization and CD103-mediated early T-cell signaling

Next, we investigated the impact of S1163A substitution on relocalization of Pxn at the contact zone of transfected JTag T cells with rE-cadherin-Fc–coated beads using the same CD103-GFP constructs used above. Pxn was strongly polarized at the contact zone with E-cadherin-Fc–coated beads when JTag T cells were transfected with the CD103-WT-GFP molecule (Fig. 4D). As expected, this polarization was inhibited by saracatinib (Supplementary Fig. S4A). Analyzing the different CD103–GFP mutants, we found that neither CD103-Δ2 nor CD103–S1163A was able to recruit Pxn at the contact area (Fig. 4D).

We finally questioned whether S^{1163} in the CD103 cytoplasmic domain was necessary for CD103-dependent early T-cell signaling by monitoring the Ca^{2+} response triggered by a combination of rE-cadherin-Fc and low doses of anti-CD3 mAb in JTag T cells transfected with the different constructs. As expected, a strong calcium response was obtained with cells transfected with CD103-WT, CD103-Δ3 and CD103-S1163D fusion proteins (Supplementary Fig. S4B). In contrast, only a weak Ca^{2+} increase was observed with CD103-Δ2. Notably, CD103–S1163A substitution had no effect on calcium response, suggesting that the structural integrity of the ES^{1163}IRKAQL motif, rather than the phosphorylation status of S^{1163}, is important for CD103-mediated early T-cell signaling. These results further support the conclusion that the CD103-ESIRKAQL intracellular motif is required for binding Pxn and initiating CD103 outside-in signaling.

Discussion

In this report, we show that the CD103 integrin is indispensable for TCR-mediated $CD8^+/CD103^+$ T_{RM} activities through the α_E chain cytoplasmic domain, and that a phosphorylatable Ser at position 1163 in the ES^{1163}IRKAQL motif of the subunit tail plays an important role in CD103 functions. We also show that the Pxn scaffold protein is involved in CD103 outside-in signaling. Indeed, engagement of CD103 with plastic-bound rE-cadherin-Fc on $CD8^+/CD103^+$ T_{RM} cells freshly isolated from human lung tumors and tumor-specific CTL clones promotes Pxn phosphorylation and binding to the CD103 cytoplasmic tail. Moreover, we found that inhibition of Pxn phosphorylation or its knockdown resulted in blockade of CD103-dependent T_{RM} functions by inhibiting both CD103 clustering and intracellular signaling, leading to cytotoxic granule polarization and exocytosis. Thus, we conclude that the α_E-subunit intracellular domain of CD103 triggers signals that control T_{RM} adhesion and migratory behavior, as well as lytic activity, cytokine release and T-cell recruitment with epithelial tumor islets, through a Pxn-dependent pathway. Consistently, we had previously reported that knockdown of E-cadherin in epithelial cancer cells blocked CD103 recruitment at the IS and, concomitantly, cytolytic granule relocalization and subsequent exocytosis (1).

Pxn exerts important functions in lymphoid cells, working as a signaling adaptor after its binding to integrin subunits (32). Pxn localizes to focal adhesions and mediates scaffolding activities by recruiting numerous structural and signaling proteins. This phosphoprotein has also been shown to bind to the α_4 integrin subunit tail (23, 24). In this case, two critical specific residues (Glu^{983} or Tyr^{991}) in a conserved 9-aa region of the α_4 cytoplasmic domain have been identified as being sufficient for Pxn binding and downstream cell spreading and migratory activities induced via the integrin. Similarly, our results show that the α_E cytoplasmic domain of the CD103 integrin contains an 8-aa region, ES^{116}IRKAQL, required for Pxn binding, CD103 polarization and lysosome accumulation at the contact zone between T cells and E-cadherin-Fc–coated beads. They also demonstrate the key role played by Ser^{1163} in this region for controlling these signaling events.

In additional experiments, we found that deletion of the whole ES^{1163}IRKAQL motif suppressed the T-cell Ca^{2+} response induced after CD3 triggering and amplified by costimulation with immobilized rE-cadherin-Fc molecules. This suggests that the ESIRKAQL sequence is required for CD103-costimulatory activity during TCR engagement. In contrast, a S1163A substitution had no effect on the Ca^{2+} response, suggesting that phosphorylation of S^{1163} is not required for this function. This discrepancy is reminiscent of what has been found with the $NITY^{759}$ motif of the β_3 integrin cytoplasmic domain. In this case, the structural integrity of this motif was required for optimal β_3 post-ligand binding events, whereas Tyr^{759} was required for β_3-mediated cytoskeleton reorganization and tyrosine phosphorylation of FAK and Pxn (33). Notably, none of the α_E cytoplasmic domain mutations generated in the present study affected the receptor-ligand interaction, indicating that the

phosphorylation status of S^{1163} in the ESIRKAQL motif is dispensable for CD103-E-cadherin interaction, but indispensable for CD103-mediated tyrosine phosphorylation of Pxn and CD103 integrin outside-in signaling effects.

Pyk2 is a protein tyrosine kinase (PTK) that interacts with several signaling and cytoskeletal molecules, such as Src family PTK and Pxn (34–37). Pyk2 plays a major role in regulating cell adhesion and migration (38, 39). It is also essential for LFA-1–mediated CD8 T-cell adhesion and migration, and a deficiency in Pyk2 resulted in a specific loss of short-lived effector CD8 T cells (40). This tyrosine kinase also contributes to CTL migration by regulating detachment of CTL at the trailing edge (41). Studies performed with human NK cells indicated that LFA-1 induced phosphorylation of Pxn and Pyk2, and that LFA-1-dependent granule polarization was blocked following Pxn knockdown (42). We show here that the interaction of CD103 on $CD8^+/CD103^+$ CTL with plastic-bound rE-cadherin-Fc resulted in phosphorylation of Pxn and Pyk2. Importantly, it has been reported that the α4-Pxn association enhanced Pyk2 and/or FAK phosphorylation, and that increased activation of Pyk2 and/or FAK is an immediate signaling event required for *trans*-regulation of LFA-1 by the α4β1 integrin (39). It is therefore tempting to speculate that the augmented phosphorylation of Pyk2 induced upon αE-Pxn ligation also stimulates LFA-1-mediated T-cell migration and functions, including in the tumor microenvironment. A role of the αE–Pxn complex in this case would be to recruit Pyk2 to sites of αE-mediated adhesion.

We report here that CD103–E-cadherin adhesion triggers phosphorylation of Pyk2 and Pxn proteins, both of which participate in the signaling properties of CD103. The Pxn N-terminus region contains five LD motifs that serve as binding sites for FAK tyrosine kinase and the integrin-linked kinase (ILK; refs. 43–45). The association of Pxn with ILK is essential for targeting ILK to focal adhesions. Involvement of ILK in both inside-out and outside-in integrin signaling (46, 47) and in β2 integrin-mediated polarization of lytic granules toward the target have been reported (48). We previously showed that the interaction of TGF-β with its receptors TGFBR on the surface of $CD8^+/CD103^+$ T cells induces recruitment and phosphorylation of ILK and its subsequent binding to the CD103 intracellular domain (13). This CD103–phospho-ILK interaction induces phosphorylation of AKT, initiating an integrin inside-out signaling leading to activation of CD103 and strengthening of CD103–E-cadherin adhesion. Therefore, it is not excluded that a Pxn–Pyk2–ILK focal adhesion complex is formed during CD103 engagement with its ligand E-cadherin.

Together, our results emphasize the crucial role of the αE-cytoplasmic domain of the CD103 integrin for the functional activities of $CD8^+/CD103^+$ T_{RM} cells infiltrating human epithelial tumor lesions. They probably explain why CD103 expression is a hallmark of this $CD8^+/CD103^+$ T_{RM} subset, as its expression is usually required for optimal anti-tumor CTL responses. Therefore, manipulating this pathway could be of great interest in the emerging field of TIL-based adoptive cell transfer therapy and optimization of immune checkpoint blockade and T-cell–based cancer immunotherapies.

Disclosure of Potential Conflicts of Interest

No potential conflicts of interest were disclosed.

Authors' Contributions

Conception and design: L. Gauthier, P. Validire, F. Mami-Chouaib
Development of methodology: L. Gauthier, S. Corgnac, G. Gros, G. Bismuth, F. Mami-Chouaib
Acquisition of data (provided animals, acquired and managed patients, provided facilities, etc.): L. Gauthier, S. Corgnac, M. Boutet, G. Gros, P. Validire, G. Bismuth, F. Mami-Chouaib
Analysis and interpretation of data (e.g., statistical analysis, biostatistics, computational analysis): L. Gauthier, S. Corgnac, M. Boutet, P. Validire, F. Mami-Chouaib
Writing, review, and/or revision of the manuscript: L. Gauthier, G. Bismuth, F. Mami-Chouaib
Administrative, technical, or material support (i.e., reporting or organizing data, constructing databases): F. Mami-Chouaib
Study supervision: F. Mami-Chouaib
Other (grant coordinator): F. Mami-Chouaib

Acknowledgments

We are grateful to Dr. M'barka Mokrani for her help with CD103-GFP constructs. We thank Prof. Michael B. Brenner and Jonathan Higgins for their kind gift of the *ITGAE* cDNA clone. We also thank Dr. Emmanuel Donnadieu, INSERM U1016, Institut Cochin Paris, for his help with calcium and tumor slice experiments, Dr. Olivier Bluteau, UMR 1009 INSERM Gustave Roussy, for his help with lentiviral constructs and the cytometry facility (Plateforme d'Imagerie-Cytométrie) of Gustave Roussy for flow-cytometry analyses.

Grant Support

F. Mami-chouaib is supported by grants from the "Association pour la Recherche sur le Cancer" (ARC; Grant number PJA20161204720), "Ligue contre le Cancer" (Comité des Yvelines, Grant number 9FI12414QLCZ), "Groupement des Entreprises Françaises dans la Lutte contre le Cancer" (GEFLUC; Grant number 2015-R15080LL) and the "Institut National du Cancer" (INCa; PLBIO016-080 Grant number 10557). S. Corgnac is supported by a grant from GEFLUC (Grant number 2016-R16180LL). L. Gauthier was a recipient of a MENRT fellowship from the French Ministry of Research and the Ligue contre le Cancer; S. Corgnac is a recipient of a fellowship from INCa and M. Boutet was a recipient of a fellowship from Gustave Roussy (SIRIC-SOCRATE).

The costs of publication of this article were defrayed in part by the payment of page charges. This article must therefore be hereby marked *advertisement* in accordance with 18 U.S.C. Section 1734 solely to indicate this fact.

Received May 19, 2017; revised August 5, 2017; accepted October 5, 2017; published OnlineFirst October 11, 2017.

References

1. Le Floc's A, Jalil A, Vergnon I, Le Maux Chansac B, Lazar V, Bismuth G, et al. Alpha E beta 7 integrin interaction with E-cadherin promotes antitumor CTL activity by triggering lytic granule polarization and exocytosis. J Exp Med 2007;204:559–70.
2. Franciszkiewicz K, Le Floc'h A, Boutet M, Vergnon I, Schmitt A, Mami-Chouaib F. CD103 or LFA-1 engagement at the immune synapse between cytotoxic T cells and tumor cells promotes maturation and regulates T-cell effector functions. Cancer Res 2013;73:617–28.
3. Piet B, de Bree GJ, Smids-Dierdorp BS, van der Loos CM, Remmerswaal EB, von der Thusen JH, et al. CD8(+) T cells with an intraepithelial phenotype upregulate cytotoxic function upon influenza infection in human lung. J Clin Inves 2011;121:2254–63.
4. Jiang X, Clark RA, Liu L, Wagers AJ, Fuhlbrigge RC, Kupper TS. Skin infection generates non-migratory memory CD8+ T(RM) cells providing global skin immunity. Nature 2012;483:227–31.
5. Mackay LK, Stock AT, Ma JZ, Jones CM, Kent SJ, Mueller SN, et al. Long-lived epithelial immunity by tissue-resident memory T (TRM) cells in the

absence of persisting local antigen presentation. Proc Natl Acad Sci U S A 2012;109:7037–42.
6. Mueller SN, Mackay LK. Tissue-resident memory T cells: local specialists in immune defence. Nat Rev Immunol 2016;16:79–89.
7. Turner DL, Farber DL. Mucosal resident memory CD4 T cells in protection and immunopathology. Front Immunol 2014;5:331.
8. Mackay LK, Minnich M, Kragten NA, Liao Y, Nota B, Seillet C, et al. Hobit and Blimp1 instruct a universal transcriptional program of tissue residency in lymphocytes. Science 2016;352:459–63.
9. Webb JR, Milne K, Watson P, Deleeuw RJ, Nelson BH. Tumor-infiltrating lymphocytes expressing the tissue resident memory marker CD103 are associated with increased survival in high-grade serous ovarian cancer. Clin Cancer Res 2014;20:434–44.
10. Djenidi F, Adam J, Goubar A, Durgeau A, Meurice G, de Montpreville V, et al. CD8+CD103+ tumor-infiltrating lymphocytes are tumor-specific tissue-resident memory T cells and a prognostic factor for survival in lung cancer patients. J Immunol 2015;194:3475–86.
11. Workel HH, Komdeur FL, Wouters MC, Plat A, Klip HG, Eggink FA, et al. CD103 defines intraepithelial CD8+ PD1+ tumour-infiltrating lymphocytes of prognostic significance in endometrial adenocarcinoma. Eur J Cancer 2016;60:1–11.
12. Wang ZQ, Milne K, Derocher H, Webb JR, Nelson BH, Watson PH. CD103 and intratumoral immune response in breast cancer. Clin Cancer Res 201622:6290–7.
13. Boutet M, Gauthier L, Leclerc M, Gros G, de Montpreville V, Theret N, et al. TGFbeta signaling intersects with CD103 integrin signaling to promote T-lymphocyte accumulation and antitumor activity in the lung tumor microenvironment. Cancer Res 2016;76:1757–69.
14. Le Floc'h A, Jalil A, Franciszkiewicz K, Validire P, Vergnon I, Mami-Chouaib F. Minimal engagement of CD103 on cytotoxic T lymphocytes with an E-cadherin-Fc molecule triggers lytic granule polarization via a phospholipase Cgamma-dependent pathway. Cancer Res 2011;71:328–38.
15. Hashimoto-Tane A, Saito T. Dynamic Regulation of TCR-Microclusters and the Microsynapse for T Cell Activation. Front Immunol 2016;7:255.
16. Hashimoto-Tane A, Sakuma M, Ike H, Yokosuka T, Kimura Y, Ohara O, et al. Micro-adhesion rings surrounding TCR microclusters are essential for T cell activation. J Exp Med 2016;213:1609–25.
17. Petit V, Boyer B, Lentz D, Turner CE, Thiery JP, Valles AM. Phosphorylation of tyrosine residues 31 and 118 on paxillin regulates cell migration through an association with CRK in NBT-II cells. J Cell Biol 2000;148:957–70.
18. Tsubouchi A, Sakakura J, Yagi R, Mazaki Y, Schaefer E, Yano H, et al. Localized suppression of RhoA activity by Tyr31/118-phosphorylated paxillin in cell adhesion and migration. J Cell Biol 2002;159:673–83.
19. Lee YC, Chang AY, Lin-Feng MH, Tsou WI, Chiang IH, Lai MZ. Paxillin phosphorylation by JNK and p38 is required for NFAT activation. Eur J Immunol 2012;42:2165–75.
20. Doucey MA, Legler DF, Faroudi M, Boucheron N, Baumgaertner P, Naeher D, et al. The beta1 and beta3 integrins promote T cell receptor-mediated cytotoxic T lymphocyte activation. J Biol Chem 2003;278:26983–91.
21. Robertson LK, Ostergaard HL. Paxillin associates with the microtubule cytoskeleton and the immunological synapse of CTL through its leucine-aspartic acid domains and contributes to microtubule organizing center reorientation. J Immunol 2011;187:5824–33.
22. Romanova LY, Mushinski JF. Central role of paxillin phosphorylation in regulation of LFA-1 integrins activity and lymphocyte migration. Cell Adh Migr 2011;5:457–62.
23. Liu S, Thomas SM, Woodside DG, Rose DM, Kiosses WB, Pfaff M, et al. Binding of paxillin to alpha4 integrins modifies integrin-dependent biological responses. Nature 1999;402:676–81.
24. Liu S, Ginsberg MH. Paxillin binding to a conserved sequence motif in the alpha 4 integrin cytoplasmic domain. J Biol Chem 2000;275:22736–42.
25. Echchakir H, Dorothee G, Vergnon I, Menez J, Chouaib S, Mami-Chouaib F. Cytotoxic T lymphocytes directed against a tumor-specific mutated antigen display similar HLA tetramer binding but distinct functional avidity and tissue distribution. Proc Natl Acad Sci U S A 2002;99:9358–63.
26. Khazen R, Muller S, Gaudenzio N, Espinosa E, Puissegur MP, Valitutti S. Melanoma cell lysosome secretory burst neutralizes the CTL-mediated cytotoxicity at the lytic synapse. Nature Comm 2016;7:10823.
27. Higgins JM, Cernadas M, Tan K, Irie A, Wang J, Takada Y, et al. The role of alpha and beta chains in ligand recognition by beta 7 integrins. J Biol Chem 2000;275:25652–64.
28. El Hage F, Vergnon I, Grunenwald D, Soria JC, Chouaib S, Mami-Chouaib F. Generation of diverse mutated tumor antigen-specific cytotoxic T lymphocytes in a lung cancer patient with long survival. Oncol Rep 2005;14:763–9.
29. Mokrani M, Klibi J, Bluteau D, Bismuth G, Mami-Chouaib F. Smad and NFAT pathways cooperate to induce CD103 expression in human CD8 T lymphocytes. J Immunol 2014;192:2471–9.
30. Adair BD, Yeager M. Three-dimensional model of the human platelet integrin alpha IIbbeta 3 based on electron cryomicroscopy and x-ray crystallography. Proc Natl Acad Sci U S A 2002;99:14059–64.
31. Vinogradova O, Haas T, Plow EF, Qin J. A structural basis for integrin activation by the cytoplasmic tail of the alpha IIb-subunit. Proc Natl Acad Sci U S A 2000;97:1450–5.
32. Deakin NO, Turner CE. Paxillin comes of age. J Cell Sci 2008;121:2435–44.
33. Schaffner-Reckinger E, Gouon V, Melchior C, Plancon S, Kieffer N. Distinct involvement of beta3 integrin cytoplasmic domain tyrosine residues 747 and 759 in integrin-mediated cytoskeletal assembly and phosphotyrosine signaling. J Biol Chem 1998;273:12623–32.
34. Lev S, Moreno H, Martinez R, Canoll P, Peles E, Musacchio JM, et al. Protein tyrosine kinase PYK2 involved in Ca(2+)-induced regulation of ion channel and MAP kinase functions. Nature 1995;376:737–45.
35. Avraham S, Jiang S, Ota S, Fu Y, Deng B, Dowler LL, et al. Structural and functional studies of the intracellular tyrosine kinase MATK gene and its translated product. J Biol Chem 1995;270:1833–42.
36. Salgia R, Pisick E, Sattler M, Li JL, Uemura N, Wong WK, et al. p130CAS forms a signaling complex with the adapter protein CRKL in hematopoietic cells transformed by the BCR/ABL oncogene. J Biol Chem 1996;271:25198–203.
37. Gismondi A, Bisogno L, Mainiero F, Palmieri G, Piccoli M, Frati L, et al. Proline-rich tyrosine kinase-2 activation by beta 1 integrin fibronectin receptor cross-linking and association with paxillin in human natural killer cells. J Immunol 1997;159:4729–36.
38. Rumsey LM, Teague RM, Benedict SH, Chan MA. MIP-1alpha induces activation of phosphatidylinositol-3 kinase that associates with Pyk-2 and is necessary for B-cell migration. Exp Cell Res 2001;268:77–83.
39. Rose DM, Liu S, Woodside DG, Han J, Schlaepfer DD, Ginsberg MH. Paxillin binding to the 4 integrin subunit stimulates LFA-1 (integrin alpha L beta 2)-Dependent T cell migration by augmenting the activation of focal adhesion kinase/proline-rich tyrosine kinase-2. J Immunol 2003;170:5912–8.
40. Beinke S, Phee H, Clingan JM, Schlessinger J, Matloubian M, Weiss A. Proline-rich tyrosine kinase-2 is critical for CD8 T-cell short-lived effector fate. Proc Nat Acad Sci U S A 2010;107:16234–9.
41. Cheung SM, Ostergaard HL. Pyk2 controls integrin-dependent CTL migration through regulation of de-adhesion. J Immunol 2016;197:1945–56.
42. March ME, Long EO. beta2 integrin induces TCRzeta-Syk-phospholipase C-gamma phosphorylation and paxillin-dependent granule polarization in human NK cells. J Immunol 2011;186:2998–3005.
43. Brown MC, Perrotta JA, Turner CE. Identification of LIM3 as the principal determinant of paxillin focal adhesion localization and characterization of a novel motif on paxillin directing vinculin and focal adhesion kinase binding. J Cell Biol 1996;135:1109–23.
44. Nikolopoulos SN, Turner CE. Actopaxin, a new focal adhesion protein that binds paxillin LD motifs and actin and regulates cell adhesion. J Cell Biol 2000;151:1435–48.
45. Nikolopoulos SN, Turner CE. Integrin-linked kinase (ILK) binding to paxillin LD1 motif regulates ILK localization to focal adhesions. J Biol Chem 2001;276:23499–505.
46. Grashoff C, Aszodi A, Sakai T, Hunziker EB, Fassler R. Integrin-linked kinase regulates chondrocyte shape and proliferation. EMBO Rep 2003;4:432–8.
47. Stevens JM, Jordan PA, Sage T, Gibbins JM. The regulation of integrin-linked kinase in human platelets: evidence for involvement in the regulation of integrin alpha 2 beta 1. J Thromb Haemost 2004;2:1443–52.
48. Zhang M, March ME, Lane WS, Long EO. A signaling network stimulated by beta2 integrin promotes the polarization of lytic granules in cytotoxic cells. Sci Signal 2014;7:ra96.